NMR Relaxation and Pulsed Gradient NMR Diffusion Measurements of Ultrasonically Devulcanized Poly(dimethylsiloxane)

Sang E. Shim,[†] Jennifer C. Parr,[‡] Ernst von Meerwall,*[,‡,§,||] and Avraam I. Isayev[†]

Departments of Polymer Engineering, Physics, Polymer Science, and Chemistry, The University of Akron, Akron, Ohio 44325

Received: March 5, 2002; In Final Form: August 29, 2002

We report ^{1}H NMR transverse relaxation and pulsed-gradient spin−echo self-diffusion measurements at 70 °C in poly(dimethylsiloxane) (PDMS) rubber before and after cross-linking, and after subsequent devulcanization by intense ultrasound. The effort serves the purpose of characterizing at a molecular level this novel method of rubber recycling. Relaxation spectra extracted from the transverse magnetization decays display three distinct components, which are further refined by a direct fit. The components are attributed to entangled and cross-linked networks; light sol and dangling network fragments; and oligomers including 4% of an unreactive trace. Ultrasound produces extractable sol strongly dependent on feed rate and transducer amplitude. Our results vary monotonically with the amount of sol: all three mobilities (T_2) and the amounts of the two most mobile fractions increase with sol content, but the diffusion rates decrease slightly, due to the production of higher molecular weight sol. Data from our earlier NMR studies of ultrasound devulcanization of styrene−butadiene and natural rubber shows strong similarities with the present results. The main difference appears to be a greater extent of loosely attached network fragments in PDMS.

Introduction

The use of nuclear magnetic resonance (NMR) in furthering the understanding of molecular structure and dynamics of polymers is well established;[1−5] poly(dimethylsiloxane)s have been the polymers of choice in a number of such investigations.[6−14] The longitudinal and transverse NMR relaxation behavior of poly(dimethylsiloxane)s of various molecular weights, from mobile liquids to gum, and for cross-linked rubbery material, has been reported over a wide temperature range.[9,15−17] The spin−spin relaxation times (T_2) increase monotonically with increasing temperature over much of the range of interest. This increase is approximately linear except for discontinuities at the glass transition (near −123 °C) and at the crystalline melting point (−50 °C)[9,14] Two minima and a discontinuity are observed in the spin−lattice relaxation time T_1. The high-temperature T_1 minima near the melting point are attributed to stretching and flexing motions of the PDMS chains due to thermally activated motions of the methyl group. The T_1 discontinuity is found to be due to melting.[16] The shape of the transverse relaxation decay, as well as the magnitude and temperature-dependence of T_2 and, to a much lesser extent, T_1, are dependent on molecular weight,[17] reflecting complex thermal motions of the dimethylsiloxane chains as recorded by the magnetic dipole interaction within and between the methyl groups of protons.[9,15]

Cross-links and entanglements both result in similar substantial decreases in T_2, and in the disappearance of the discontinuity.[9] In physical or chemical networks containing additional, unentangled, material (e.g., in broadly polydisperse melts), the transverse relaxation decay displays a distribution of rates, most typically bimodal.[17] The presence of particulate filler, e.g., silica particles,[14] leaves this observation unaffected[9] but results in a further modest reduction in both T_1 and T_2.

Translational diffusion of small molecules is manifested in NMR relaxation as a lengthening of T_2, and semiquantitative estimates of the diffusion coefficent[18] may be obtained from this effect. In the presence of solvents, diluents, extender oils, plasticizers, and reagents dispersed in polymeric media, or in blends with a wide molecular weight distribution, this method of extracting diffusivities becomes prohibitively cumbersome. However, the use of the pulsed-gradient spin−echo (PGSE) method,[19] requiring modifications to the pulsed NMR spectrometer, makes it possible to measure diffusion directly and precisely without partitioning the relaxation rates or requiring assumptions other than the applicability of Fick's law.[19,20] This method, too, has long been used in the study of polymeric systems.[20]

In previous publications,[21,22] a novel method of devulcanization using ultrasound irradiation at various temperatures and pressures has been described in detail. The purpose of devulcanization is to prepare the rubbery material for recycling by subsequent vulcanization. A molecular-level understanding of the effects of ultrasound exposure is indispensable in guiding and optimizing the process, but additionally confers much generally useful information about the constitution and kinetics of rubbery networks. The intense ultrasound process is known to break chemical bonds, preferentially weak cross-links, producing significant amounts of extractable sol in various types of rubber including ground rubber tires (GRT), styrene−butadiene rubber (SBR), and natural rubber (NR).[21−24] The nature of the damage to the network through ultrasound devulcanization of SBR, and the kinetics of the molecular fragments detached, have been analyzed using ^{13}C and ^{1}H NMR relaxation and ^{1}H PGSE diffusion measurements.[25] In that study,

* Corresponding author. Tel.: 330-972-5904. Fax: 330-972-5290. E-mail: evm@physics.uakron.edu.
[†] Department of Polymer Engineering.
[‡] Department of Physics.
[§] Department of Polymer Science.
[||] Department of Chemistry.

10.1021/jp0257247 CCC: $22.00
Published on Web 10/17/2002

the two major components of interest were extractable sol and unextractable gel. The extractable sol includes unreacted polymer molecules and oligomers, solvents, impurities, and larger detached network fragments. Unextractable gel represents chemical network remnants, including loosely attached polymer chains. However, NMR relaxation interprets entangled molecules or fragments as part of the network (chemical plus physical) rather than as part of the sol. Thus, this[25] and subsequent studies make a clear distinction between the entire chemically extractable sol and that portion ("light sol") arising only from unentangled unattached molecules. The fraction of light sol was obtained by fitting the experimentally obtained T_2 decay with a simple two-component model, which adequately represented the data.

As for the diffusion of the lighter sol components, it was found that the mean diffusivity of the light sol in devulcanized SBR decreased with increasing ultrasound amplitude, suggesting that the molecular mobility of devulcanized rubber is decreased by stiffening of the molecular chains. This observation was in accord with the observed changes[25] in ^{13}C T_2, and yielded to an analysis in terms of the Williams−Landel−Ferry free-volume theory[26] using the measured glass transition temperatures. Whereas ^{13}C NMR spin−spin relaxation was clearly dominated by intrachain kinetics, ^1H T_2 showed an opposite trend, being related to the abundance and mobility of smaller sol molecules. The contrast between the carbon and proton NMR results offered much-needed insight into the underlying complementarity of the motional attributes and spatial scales in this system. Analogous observations in devulcanized NR[27] provided similar information but required a slightly more complex interpretation.

Recently, ultrasound devulcanization has been successfully applied to poly(dimethylsiloxane).[28,29] In an effort to improve our understanding of the devulcanization process we undertook a complementary study of the molecular mobility of the entanglement and cross-link network and the production, segmental mobility, and diffusion rate of the smaller sol molecules. This investigation was again conducted using proton-pulsed NMR relaxation and PGSE diffusion measurements. Preliminary oral reports of this work have been given.[30] We find that, as ultrasound irradiation is intensified or extended in duration, our results permit useful inferences about the changing mass-distribution of sol molecules, and the increasing disorganization and destruction of the cross-linked network. These analytical methods document the relative inefficiency of ultrasound in promoting further fractionation of the detached molecular fragments, and provide sufficient detail to distinguish between the effect on PDMS vulcanizates of the intensity and the duration of ultrasound exposure.

Experimental Section

Network Preparation. Polymeric networks were prepared by cross-linking poly(dimethyl siloxane) PDMS SE 64 made by the General Electric Company. The starting material had a weight-average molecular weight $M_w = 4.14 \times 10^5$ and a number-average molecular weight $M_n = 2.34 \times 10^5$ as measured by gel permeation chromatography, GPC. It contained 0.6 mol % vinyl groups. Dicumyl peroxide (DCP), LUPEROX 500R (Pennwalt Corp.), was used as the curative. DCP (0.5 phr) was added to PDMS on the two-roll mill at 25 °C. After mixing, the compounds were pre-cured at 170 °C in a compression molding press (Wabash) in the form of $260 \times 260 \times 12$ mm^3 slabs, then post-cured in a ventilated oven at 200 °C for 2 h. The vulcanized sheets were ground into particles using a Nelmor grinding machine with a 5 mm screen.

Ultrasound Devulcanization. These ground cured PDMS particles were fed into a rubber extruder with an ultrasound die attachment[22] to achieve devulcanization. The temperature of the extruder barrel was set at 180 °C. The screw speed was 20 rpm and the cooling water flow rates for both die and horn were set at 0.09 m^3/h. The gap between the flat face of the horn and the die exit surface was 0.63 mm, and the flow rates were 0.32 (2.5), 0.63 (5.0), and 1.26 g/s (10 lb/h). A 3000 W ultrasound power supply, a converter, and a booster were used to provide longitudinal vibrations to the horn at a frequency of 20 kHz. The amplitudes at the transducer face of the ultrasonic wave were 5, 7.5, and 10 μm. The devulcanized PDMS exiting from the die was collected for investigation.

Characterization. Gel fractions of the vulcanized and devulcanized samples were measured by Soxhlet extraction, using benzene as the solvent. Cross-link densities of the gel were determined by the swelling method. The cross-link density, n_c, was calculated using the Flory-Rehner equation[31] as described elsewhere.[29]

The molecular weights of the virgin silicone melt and of the sol of devulcanized PDMS were investigated by GPC. The apparatus consisted of a Waters 510 GPC, a Differential Viscotek 100 viscometer, and a Waters 410 differential refractometer. Three Waters Styragel high-resolution columns were used. The calculation of molecular weight was based on a universal calibration performed by using the Aldrich Polystyrene Standard kit consisting of 13 standards. The solvent used was THF; the desired dilution of 3 mg/mL was obtained by dissolving a 0.09 g sample in 30 mL of THF at room temperature for about 24 h. The GPC was set to a temperature of 30 °C, a flow rate of 1.0 mL/min and an injection volume of 0.1 mL. The sample was filtered and then injected into the column.

NMR T_2 Relaxation Measurements and Data Analysis. All NMR and diffusion measurements were conducted in the ^1H NMR at 70 °C, the elevated temperature being chosen to accelerate molecular/segmental motions and accentuate differences between gel and sol, and also to permit convenient comparison with our previous NMR study of other types of rubber conducted at this temperature. The 33 MHz modified Spin-Lock CPS-2 spectrometer with its attachments to permit diffusion measurements, and our data interpretation methods, have been comprehensively described elsewhere in their early implementation.[32,33] The pulse sequence employed was the standard principal Hahn spin−echo sequence $90°-\tau-180°-\tau-$echo, and the echo height $A(2\tau)$ was measured on-resonance after signal averaging over six passes. For optimum audio signal linearity, the spectrometer performed single-channel radio frequency (rf) phase-sensitive detection. Pulse spacing τ was adjusted between 0.1 ms and at least 60 ms in 30 or more steps, until the echo signal-to-noise ratio was less than 2, i.e., the echo amplitude had fallen to less than 0.5% of its initial value. This procedure ensured that the tail of the echo decay, from which the light sol fraction and sol mobility are inferred, is adequately characterized. Optimization of magnetic field homogeneity combined with the relatively low sol diffusion coefficients (see below) ensured that the T_2 values measured with the two-pulse sequence were not falsified by diffusional artifacts.[34]

The echo decay was initially analyzed in terms of a two-component relaxation model,which had served well in previous polymer-related work,[25,27,35,36] including devulcanization studies by this laboratory. However, it was found that for PDMS the fit to our data was uniformly unacceptable. To guide the refinement of the model, a generalized spectral decomposition

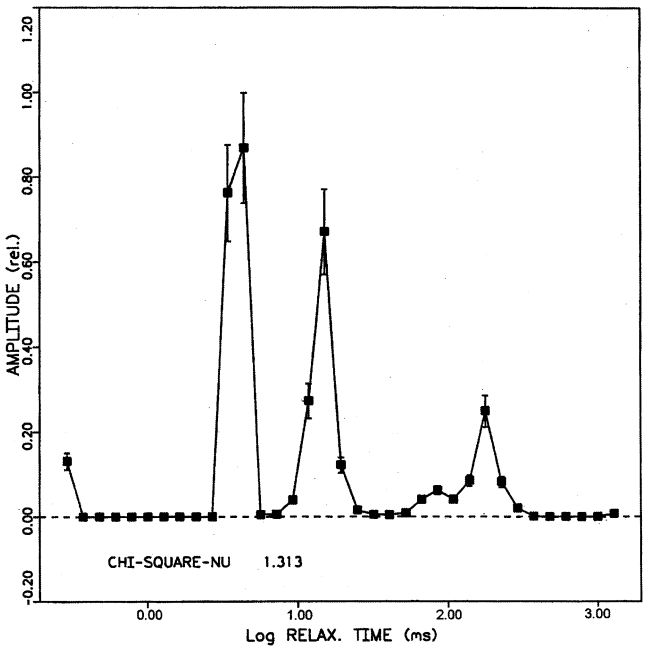

Figure 1. Spectral decomposition (40 components) of the transverse proton magnetization decay at 70 °C in PDMS devulcanized at the feed rate of 0.32 g/s, ultrasound amplitude of 10 μm, and at a gap distance of 0.63 mm.

of the echo attenuation was performed. It has the form

$$\frac{A(2\tau)}{A(0)} = \sum_{j=1}^{n} p_j^{\,2} \exp\left[-\left(\frac{2\tau}{T_{2j}}\right)^{b_j}\right] \tag{1}$$

where $b_j = 1 + \exp[-(T_{2j}/T_{2c})]$, with $T_{2c} \approx 0.3$ ms; this exponent describes the observed transition from a Gaussian to an exponential decay as T_2 increases through T_{2c}.

The desired n parameters are the amplitudes p_j^2 of the relaxation time components T_{2j} chosen to be equally spaced logarithmically in time; n was set near 70% of the number of data points, not to exceed $n = 40$. The use of a nonlinear least-squares curve fitting program[37] was dictated by the need to fit squared parameters in order to avoid some otherwise inevitable unacceptable negative component amplitudes.

Figure 1 shows the spectral decomposition of the transverse proton magnetization decay at 70 °C for PDMS devulcanized at the feed rate of 0.32 g/s, ultrasound amplitude of 10 μm, and at a gap clearance of 0.63 mm. The fit is acceptable, and suggests that the transverse magnetization decays should be well described in terms of three components. (A minor component at the shortest time, present in most samples including the melt, is attributed to a slight detector phase mismatch between the free induction decay and the first echo, rather than to a trace of rigid material.) Consequently, the relaxation model ultimately employed—successfully in all cases—is given by

$$\frac{A(2\tau)}{A(0)} = f_S \exp(-2\tau/T_{2S})^E + f_L \exp(-2\tau/T_{2L}) + (1 - f_S - f_L) \exp(-2\tau/T_{2M}) \tag{2}$$

where T_{2S}, T_{2M}, and T_{2L} signify the short, medium, and long relaxation times, respectively; f_S, $(1 - f_S - f_L)$, and f_L are their relative intensities; and E is the Weibull exponent, found to vary between about 1.0 (longest T_{2S}) and 1.6 (shortest T_{2S}).

When the diffusion of light sol is to be studied, this can conveniently be done provided $T_{2L} \gg T_{2S}$, as was the case in this study, simply by operating near the optimal condition:

$$T_{2S} << 2\tau < \approx T_{2L} \quad \text{(max. sol echo, no gel echo)} \tag{3}$$

This procedure resulted here in the choice of $\tau = 20$ ms at $T = 70$ °C, and ensured that our diffusion measurements were free of distortion by (unattenuatable) echo contributions from the gel. The role of the intermediate component (T_{2M}) is more complex, and will be discussed below.

PGSE Diffusion Measurements and Data Analysis. This method is based on a spin−echo experiment, e.g., the one described above, that additionally calls for the application of a pair of magnetic field gradient pulses of magnitude G and duration δ in coordination with the rf pulse sequence. For diffusing molecular species the echo is attenuated; its amplitude is recorded as function of the gradient parameter $X = \delta^2G^2(\Delta - \delta/3)$, where the delay between the gradient pulses is $\Delta = \tau$.

For the present work, the following practices were adopted; many of these differ from those described in our initial implementation.[32] For reasons of stability and convenient access to the echo signal baseline a small steady gradient of magnitude G_o was applied throughout, and this required the addition to X of a small term[19] proportional to $G{\cdot}G_o$. In this study the parameter settings used were fixed values of $\Delta = \tau = 20$ ms; $G = 634$ G/cm; $G_o = 0.3$ G/cm, with δ varying in eight to twenty steps until the echo signal was attenuated to the background noise level, or until $\delta = 12$ ms was reached. The PGSE experiment was conducted off-resonance by −3 kHz, using the magnitude Fourier transform of the beat pattern between the phase-sensitively detected signal and the reference oscillator, integrating over the echo peak, and correcting for rms background noise. Echo height measurements were signal-averaged over six to twelve passes.

In the nonspectroscopic high-gradient version of the PGSE method employed in all cases such as ours, where chemical shift differences are unresolvable, a D distribution manifests itself as an upward concavity in the echo attenuation plots log A vs X, arising from a linear superposition of component attenuations.[19,20,32,33] When the diffusion rates are expected to display a distribution whose exact shape eludes confident prediction, the rates may be modeled as a discrete distribution calling for several components having fractional amplitudes a_i and diffusion coefficients D_i; thus the echo attenuation assumes the form

$$\frac{A(2\tau,X)}{A(2\tau,0)} = \sum_i a_i \exp(- \gamma^2 D_i X) \tag{4a}$$

where γ represents the gyromagnetic ratio of the nucleus at resonance (^{1}H). When there are only two diffusing species in the system of concern, eq 4a takes the form

$$\frac{A(2\tau,X)}{A(2\tau,0)} = f_{fast} \exp[-\gamma^2 D_{fast} X] + (1 - f_{fast}) \exp[-\gamma^2 D_{slow} X] \tag{4b}$$

where D_{fast} and D_{slow} represent the diffusivities of the two motional species, and f_{fast} denotes the echo fraction of the fast-diffusing species at $t = 2\tau$. In cases where one (typically the slower-diffusing) component displays a diffusivity distribution arising from molecular polydispersity, the second component is modeled along the lines of eq 4a, with a_i and D_i based on the M-distribution and the known scaling relation (Rouse or reptation) between molecular weight and diffusion. This com-

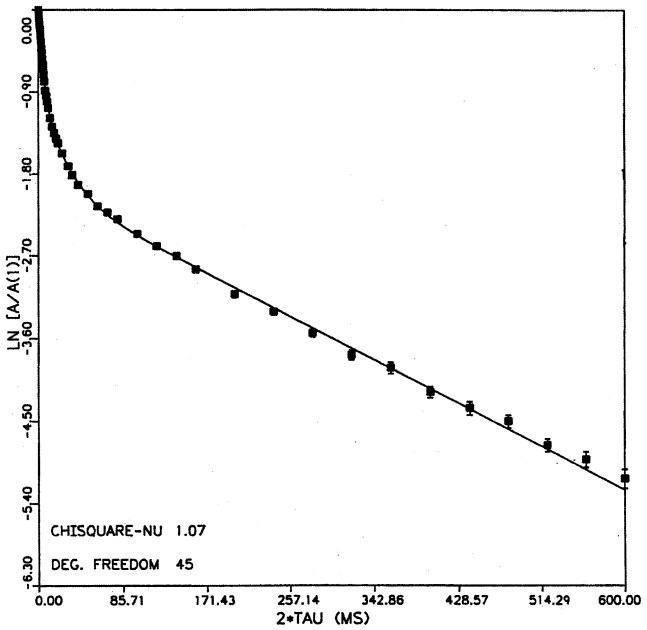

Figure 2. Transverse proton magnetization in the specimen of Figure 1, together with a successful three-component, six-parameter fit of eq 2.

plex model has been described in detail,[33] and is incorporated in the off-line PGSE data reduction code DIFUS5[38] in its current version. The adjustable parameters for this model are D_{fast}, $D(M_n)$, and f_{fast}, the polydispersity ratio M_w/M_n remaining fixed at the value supplied as input. It was found in all instances that this model after parameter adjustment adequately reproduced the diffusional echo attenuation data.

Results and Discussion

NMR Relaxation. Figure 2 shows the transverse relaxation decay data used to generate Figure 1, reanalyzed in terms of the six-parameter model of eq 2. Chi-square is further reduced, mainly because of the now larger number of degrees of freedom, a fact which ensures that the three-component description is both adequate and economical.

The same analysis was successfully carried out for all specimens studied. Figure 3 shows T_{2S}, T_{2M}, and T_{2L} plotted as function of the fraction of chemically extractable sol, the latter representing a measure of the extent of the devulcanization. Data for the pre-cure melts are included (100% "sol"). It is seen that the correlation is satisfactory, and that all component molecular mobilities are increased as a result of ultrasound exposure. Interestingly, the factor of increase is, within experimental error, the same for the three components, with the virgin melt having the highest mobilities. The relative contributions of the components to the echo, however, depend significantly on the ultrasound treatment.

This information, in the form of f_S, $f_M = (1 - f_S - f_L)$, and f_L, is shown in Figure 4, again as function of the fraction of extractable sol. The presence of a significant f_S for the virgin melt clearly confirms the conclusion reached earlier for SBR and NR that, except for minor enhancements of segmental mobility (T_{2S}), physical cross-links in the form of entanglemens are nearly indistinguishable in NMR relaxation from chemical cross-links. As ultrasound treatment generates more sol, the fraction of long and intermediate components increases substantially at the expense of the short component. In contrast to the relaxation times, here the results for the virgin melt more closely resemble those of the untreated vulcanizate rather than

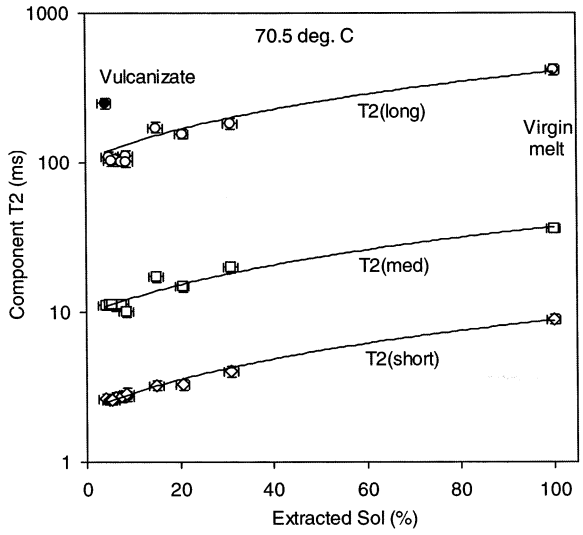

Figure 3. T_2 relaxation times of the short, medium, and long components for the series of devulcanized and virgin PDMS specimens as a function of extractable sol content.

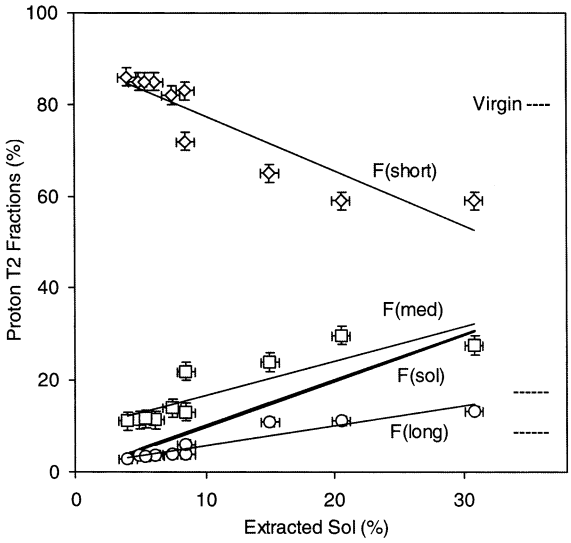

Figure 4. Dependence on sol content of the fraction of short, medium, and long T_2 relaxation time components (see Figure 3) for the series of devulcanized (symbols; solid lines) and virgin (dashed lines) PDMS specimens. Bold line represents measured sol fraction (= abscissa value).

the most vigorously devulcanized specimens, indicating that vulcanization reduces overall mobilities without significantly affecting the components' proportions, hence maintaining the shape of the magnetization decay except for a time-scaling factor.

The bold line in Figure 4 represents the extractable sol fraction itself, and its position well above f_L indicates that a substantial and increasing portion of the intermediate and perhaps short component arises from the chemically extractable material. Still, the fact that $f_L + f_M$ invariably exceeds the extractable sol fraction indicates that at least some of the intermediate (and, of course, short) component represents the unextractable material. In other words, the intermediate component must divide its origins between detached and still-attached network fragments of roughly equal segmental mobilities. On the basis of the component mobilities and relative contributions, and their dependences on sol fraction, it is now possible to assign the short component to the cross-linked and entangled network increasingly loosened and diminished by ultrasound and pen-

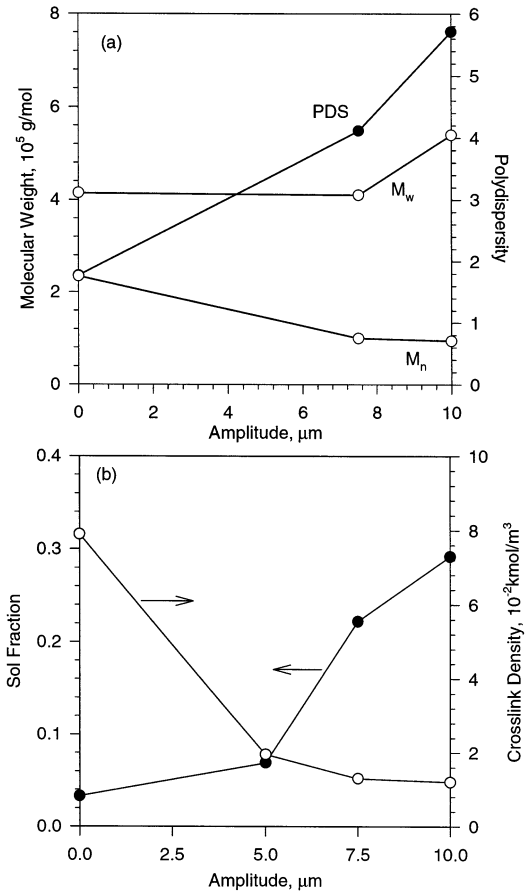

Figure 5. Molecular weights (open symbols) and polydispersity (filled symbols) of extracted sol of devulcanized PDMS (a); sol fraction (solid symbols) and cross-link density (open symbols) of devulcanized PDMS (b), shown as a function of ultrasound amplitude. The devulcanization samples were obtained at a die gap of 0.63 mm, a flow rate of 0.32 g/s, and a barrel temperature of 180 °C.

etrated by highly mobile and diffusing sol. Because of its distinct separation from the intermediate component, the long component must arise from the unreactive oligomers present in all specimens irrespective of treatment, plus relatively small increments of very light, unbranched, material produced by ultrasound. It appears that ultrasound exposure of PDMS degrades the network by detaching molecular fragments of at least intermediate size, but leaves copious amounts of fragments dangling. Significantly, ultrasound seems inefficient at further tearing of such fragments into oligomeric dimensions, or at detaching oligomer-size material directly from the network. These conclusions will be confirmed and further elaborated by the analysis of the diffusion data as well as by chemical analysis of the extracted sol.

Analysis of Gel and Extracted Sol. The molecular weight and polydispersity of the sol extracted from several specimens of devulcanized rubber is shown in Figure 5a as a function of the ultrasound amplitude. Both the average molecular weight M_w and the polydispersity in the sol of devulcanized PDMS increase with increasing ultrasound amplitude, while the amount of extractable sol increases, and the cross-link density of the network after extraction decreases, with increasing ultrasound intensity (Figure 5b). These observations directly confirm the earlier interpretation that severe devulcanization conditions at higher ultrasound amplitude produce considerable amounts of extractable sol mainly of larger size, but also including a few oligomers, and that the remaining chemical network is substantially degraded.

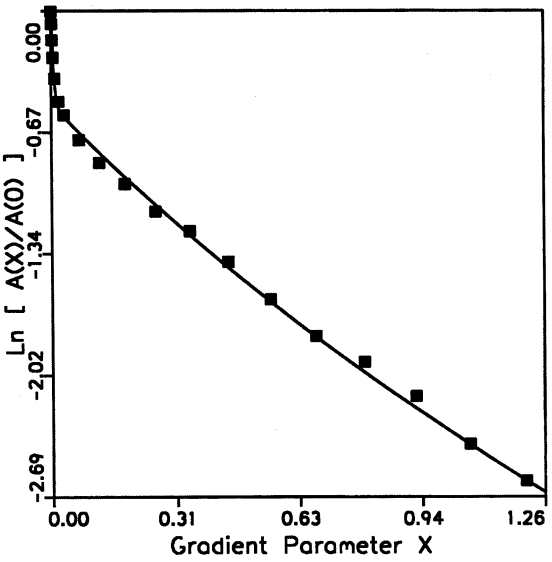

Figure 6. Diffusional spin−echo attenuation in a PDMS network devulcanized at a barrel temperature of 180 °C, a die gap of 0.63 mm, and a flow rate of 0.32 g/s. Curve represents eq 4b with the polydispersity feature enabled for the slow component, fitted to data by optimizing D_{fast}, $D(M_n)$, and f_{fast}; M_w/M_n was set to 1.5.

Diffusion of Light Sol Components. Figure 6 shows an example of diffusional echo attenuation data in a devulcanized specimen together with a fit of eq 4b modified to represent a polydisperse slow component, as described above. The rf pulse spacing time τ was set to 20 ms, making the effective diffusion time $\tau - \langle d \rangle/3 = 17.7$ ms. This choice of τ resulted in the observation of essentially the full intensity of the long-T_2 component, together with modest but significant contributions from the intermediate component, while avoiding inclusion of the short component. Under these conditions all oligomeric material and most of the unentangled detached fragments were accessible to diffusional study.

Of interest here and in all other specimens examined is the observation of a sharply bimodal diffusivity spectrum. The data suggests that the fast-diffusing portion arises from the oligomeric material relaxing at T_{2L}, and that the lower-diffusivity portion originates with unentangled molecular fragments, i.e., nonoligomeric polydisperse light sol relaxing at T_{2M}. However, this simple picture is quantitatively inconsistent and needs to be modified.

It should be mentioned that the polydispersity index M_w/M_n, required to reproduce the echo attenuations for the slowly diffusing component, while not optimized in our fits, tended to be consistent with values near 1.5. The chemically measured values for the extracted sol shown in Figure 5a are much larger, because they additionally include both the oligomeric portion of the distribution (D_{fast}) as well as the entangled fractions of the sol excluded from the PGSE data.

Identical measurements were carried out for the entire series of samples, with results differing only in quantitative detail. To check for complete attenuation of the spin−echo, measurements at larger $\Delta = \tau$ and with the stimulated-echo sequence[39] were also made for several samples and succeeded fully, but with correspondingly decreased signal amplitude and precision in the deduced diffusivity. Complete echo attenuation is a direct evidence that the conditions of eq 3 were met, no gel echo being included in the diffusion measurement. No dependence of either D_{fast} or $D(M_n)$ on diffusion time was observed, attesting to the expected adherence to Fick's first law, hence of absence of spatial restrictions to diffusion.

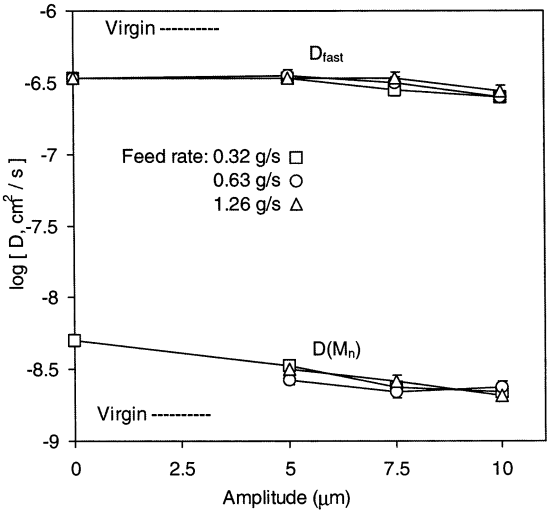

Figure 7. Diffusivity D_{fast} of the fast component (top) and mean diffusivity D(M_n) of the slow-diffusing species (bottom) in devulcanized (symbols; solid lines) and virgin (dashed lines) PDMS as a function of ultrasound amplitude.

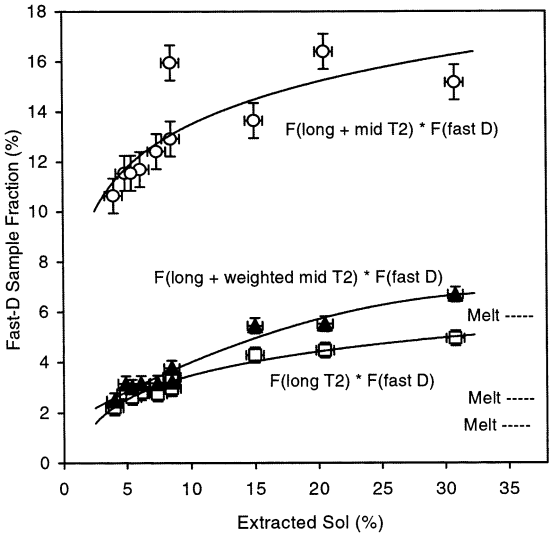

Figure 8. Approximate portion (proton fraction) of the devulcanized (symbols, solid lines) and virgin melt (dashed lines) PDMS samples consisting of the fastest-diffusing molecular species. Plot combines relaxation data (Figure 4) and diffusion data (see text). Solid symbols provide the best estimate.

In Figure 7, the diffusivities D_{fast} and D(M_n) in devulcanized PDMS samples are plotted as a function of ultrasound amplitude, showing that the two rates differ by almost 2 orders of magnitude. The decrease of the diffusion rate with increase in ultrasound amplitude for the slow-moving species is greater than that of fast-moving molecules, indicating that as devulcanization conditions become more severe, copious additional unentangled sol molecules are created with masses greater than those present in the virgin melt. The analogous effect observed in SBR[25] was more pronounced than in PDMS, but additional mechanisms were found to contribute.

Changes in the diffusion coefficient may arise from one or more of three separate causes: changes in the diffusant's average molecular weight; changes in the host molecular mobility, e.g., by free volume; and changes in the diffusant/host monomeric friction constant at constant free volume, e.g., due to branching. Since the glass transition temperature measured in several of these specimens was not sensitively dependent on ultrasound exposure, substantial free-volume-based diffusivity changes would seem to be ruled out. However, the effects of molecular weight and of branching in the light sol molecules produced by ultrasound are not separable in the present experiment. Still, the decrease of D_{fast} with increasing sol fraction, although less than that of D(M_n), indicates that even the smallest diffusing species sense the retarding effects of the production of large amounts of slower-moving material, either as host materials for the diffusion of the lightest species or as diffusants, via an increase of the oligomers' own average molecular weight.

Additional information on this topic is available from the fractional contribution of the fast-diffusing portion of the echo. It displays a significant decrease with increasing extractable sol fraction f_{SOL}, but this trend is not directly interpretable since τ was fixed for all diffusion measurements, whereas the components' relaxation times and their relative amplitudes, hence their contribution to the echo at $2\tau = 40$ ms, varied systematically and substantially. To obtain the proportion of the fast-diffusing species of the sample, F_{FAST}, one is led to multiply f_{fast}, the fraction of the fast-diffusing portion of the echo at 40 ms, by the fraction of the echo from that species contributing a signal at 40 ms. The latter quantity is imperfectly defined, consisting mainly of f_L but including an unknown portion of f_M. Figure 8 plots this product as function of f_{SOL}. The lower trace (open squares) assumes, unreasonably, that none of the molecules characterized by T_{2M} are diffusing, whereas the upper trace (open circles) even more unreasonably assumes that all of the T_{2M} material is free to diffuse. The most promising, but still approximate, procedure is to augment f_L by a T_2-weighted portion of f_M, obtaining

$$F_{FAST} = f_{fast}(2\tau)\, f_L'(2\tau) \tag{5}$$

with

$$f_L'(2\tau) = f_L + f_M \exp[2\tau(T_{2L}^{-1} - T_{2M}^{-1})] \quad (2\tau = 40 \text{ ms})$$

This estimate is shown as the filled symbols in Figure 8. It is clear that while the sol fraction rises by a factor near 30 as ultrasound exposure is intensified, the fraction of the sample diffusing at the highest rates increases by a factor of 3 or less. Since the fast-diffusing material is also present and distinguishable in the melt and in the vulcanizate (where it is the only diffusing echo component discernible at 40 ms), it must initially consist of small, largely unreactive, molecular species. The additional amount of this fraction produced by devulcanization even under the harshest conditions encountered here never constitutes more than some 4% of the protons in the sample, and hence no more than 15% of the added extractable sol. Thus, it is clear that ultrasound devulcanization is highly inefficient at producing molecular fragments as small as oligomers. Given the force gradients available via ultrasound, we speculate that there is an intensity-dependent critical dimension of the molecular fragments below which the force is no longer sufficient to break main-chain bonds due to the chains' ability to respond rapidly to tensile stress. The copious amounts of sol generated by ultrasound tend to have intermediate or higher molecular weights, both above and below the critical value M_c for the onset of entangled diffusion, and probably with various degrees of short branching.

Conclusions

We have complemented our earlier NMR relaxation and diffusion study of the ultrasound devulcanization method in SBR and NR with an ^{1}H NMR transverse relaxation and PGSE

diffusion study in samples based on moderately polydisperse PDMS of weight average molecular weight of 4.14×10^5 g/mol. The T_2 relaxation and diffusion rate of PDMS samples devulcanized at various ultrasound amplitudes and feed rates were studied. To obtain agreement with the transverse relaxation decay data it was necessary to invoke a three-component model, arising from three distinct motional species; the diffusion spectrum characterized the two more mobile species in detail. Our findings may be summarized as follows:

(1) Proton NMR relaxation in PDMS sees entangled molecules as network (gel), but interprets unentangled unattached segments as sol. This observation is in keeping with our earlier results for SBR and NR. NMR sol also includes unreactive oligomers.

(2) Vulcanization does not significantly link the lowest-M fractions.

(3) Devulcanization produces more sol, both entangled and unentangled ($M \leq M_c$), likely of various degrees of branching, in copious amounts dependent on ultrasound power, and weakly dependent on cavity gap width. It also greatly increases the amount of loosely attached network fragments.

(4) Devulcanization increases the mobility (T_2) of the gel segments, of the added light sol, and of the unreacted oligomers, by equal factors, closely correlated with the amount of extractable sol. The T_2 spectrum is more complex in PDMS than in SBR and NR.

(5) Devulcanization decreases the diffusivity of the light sol and, to a smaller extent, of the oligomer remnants. These changes reflect a broad sol M-distribution, a conclusion directly confirmed by sol characterization.

(6) Devulcanization was earlier shown to increase main-chain stiffness of SBR via changes in bonding ratios, and to result in mesoscale inhomogeneities in molecular architecture. A similar phenomenon is expected to occur in PDMS, but was not directly confirmed.

(7) The combination of transverse NMR relaxation and PGSE diffusion measurements makes possible the extraction of significant information not obtainable in other ways. In particular, detailed insights into the details of segmental and molecular kinetics and dynamics should provide substantial guidance in optimizing the techniques for recycling these and other ultrasound-devulcanized rubbers.

Work in progress in this laboratory includes an examination of particulate-filled rubbers including PDMS, and a study of the differences between original vulcanizates and material subjected to revulcanization after intensive ultrasound exposure.

Acknowledgment. The portion of the work conducted in the Institute of Polymer Engineering is supported by Grant DMI-084740 from the National Science Foundation, Division of Engineering, to whom we express our appreciation.

References and Notes

(1) Slichter, W. P. *Adv. Polym. Sci*. **1958**, *1*, 35.
(2) Sauer, J. A.; Woodward, A. E. *Rev. Modern Phys*. **1960**, *32*, 88.
(3) McBrierty, V. J.; Douglass, D. C. *Macromol. Rev*. **1981**, *16*, 295.
(4) Spiess, H. W. *Adv. Polym. Sci*. **1985**, *66*, 23.
(5) Fedotov, V. D.; Schneider, H. *Structure and Dynamics of Bulk Polymers by NMR-Methods*; Springer-Verlag: Berlin, 1989.
(6) Huggins, C. M.; St. Pierre, L. E.; Bueche, A. M. *J. Phys. Chem*. **1960**, *64*, 1304.
(7) Huggins, C. M.; St. Pierre, L. E.; Bueche, A. M. *J. Polym. Sci.: Part A* **1963**, *1*, 2731.
(8) Powles, J. G. *Polymer* **1960**, *1*, 219.
(9) Powles, J. G.; Hartland, A.; Kail, J. S. E. *J. Polym. Sci*. **1961**, *55*, 361.
(10) Litvinov, V. M.; Spiess, H. W. *Makromol. Chem*. **1991**, *192*, 3005.
(11) Cuniberti, C. *J. Polym. Sci. A-2* **1970**, *28*, 2051.
(12) Folland, R.; Charlesby, A. *Int. J. Radiat. Phys. Chem*. **1976**, *8*, 555.
(13) Folland, R.; Charlesby, A. *Int. J. Radiat. Phys. Chem*. **1977**, *10*, 61.
(14) Kusumoto, H.; Lawrenson, I. J.; Gutowsky, H. S. *J. Chem. Phys*. **1960**, *32*, 724.
(15) Powles, J. G.; Hartland, A. *Nature* **1960**, *186*, 26.
(16) Burnett, L. J.; Rottler, C. L.; Laughon, D. H. *J. Polym. Sci.: Polym. Phys. Ed.* **1978**, *16*, 341.
(17) Folland, R.; Steven, J. H.; Charlesby, A. *J. Polym. Sci.: Polym. Phys. Ed.* **1978**, *16*, 1041.
(18) McBrierty, V. J. M.; Douglas, D. G. *Phys. Rep*. **1980**, *63*, 61; *Macromol. Rev*. **1981**, *16*, 295.
(19) Stejskal, E. O.; Tanner, J. E. *J. Chem. Phys*. **1965**, *42*, 288.
(20) See, for example, von Meerwall, E. *Rubber Chem. Technol*. **1985**, *58*, 527.
(21) Isayev, A. I.; Chen, J.; Tukachinsky, A. *Rubber Chem. Technol*. **1995**, *68*, 267.
(22) Tukachinsky, A.; Schworm, D.; Isayev, A. I. *Rubber Chem. Technol*. **1996**, *69*, 92.
(23) Levin, V. Yu.; Kim, S. H.; Isayev, A. I. *Rubber Chem. Technol*. **1997**, *70*, 120.
(24) Tapale, M.; Isayev, A. I. *J. Appl. Polym. Sci*. **1998**, *70*, 2007.
(25) **)** Levin, V. Yu.; Kim, S. H.; Isayev, A. I.; Massey, J.; von Meerwall, E. *Rubber Chem. Technol*. **1996**, *69*, 107; and Johnston, S. T.; Massey, J.; von Meerwall, E.; Kim, S. H.; Levin, V. Yu.; Isayev, A. I. *Rubber Chem. Technol*. **1997**, *70*, 183.
(26) Williams, M. L.; Landel, R. F.; Ferry, J. D. *J. Am. Chem. Soc*. **1955**, *77*, 3701.
(27) Parr, J. C.; Massey, J.; von Meerwall, E.; Hong, C.-K.; Isayev, A. *Bull. Am. Phys. Soc*. **1998**, *43*, 2158, and **1999**, *44*, 1192.
(28) Diao, B.; Isayev, A. I.; Levin, V. Y. *Rubber Chem. Technol*. **1999**, *72*, 152.
(29) Shim, S. E.; Isayev, A. I. *Rubber Chem. Technol*. **2001**, *74*, 303.
(30) Parr, J. C.; von Meerwall, E.; Shim, S. E.; Isayev, A. *Bull. Am. Phys. Soc*. **2001**, *46*, 25 and 1098.
(31) Flory, P. J.; Rehner, J., Jr. *J. Chem. Phys*. **1943**, *11*, 521.
(32) von Meerwall, E.; Ferguson, R. D. *J. Appl. Polym. Sci*. **1979**, *23*, 877.
(33) von Meerwall, E.; Palunas, P. *J. Polym. Sci., Part B: Polym. Phys. Ed*. **1987**, *25*, 1439.
(34) Meiboom, S.; Gill, D. *Rev. Sci. Instrum*. **1958**, *29*, 688.
(35) Mahoney, D.; von Meerwall, E. *J. Polym. Sci. Part B: Polym. Phys. Ed*. **1993**, *31*, 1029.
(36) Bradley, D. S.; von Meerwall, E.; Roberts, G. D.; Kamvouris, J. *J. Polym. Sci. Part B: Polym. Phys. Ed*. **1995**, *33*, 1545.
(37) von Meerwall, E. *Comput. Phys. Commun*. **1976**, *11*, 211.
(38) von Meerwall, E.; Ferguson, R. D. *Comput. Phys. Commun*. **1981**, *21*, 421.
(39) Tanner, J. E. *J. Chem. Phys*. **1970**, *52*, 2523.